THE JOURNAL OF BIOLOGICAL CHEMISTRY VOL. 284, NO. 23, pp. 15505–15516, June 5, 2009

Identification of Sequences in the Polysialyltransferases ST8Sia II and ST8Sia IV That Are Required for the Protein-specific Polysialylation of the Neural Cell Adhesion Molecule, NCAM*[S]

Received for publication, December 24, 2008, and in revised form, March 27, 2009 Published, JBC Papers in Press, March 31, 2009, DOI 10.1074/jbc.M809696200

Deirdre A. Foley[1], **Kristin G. Swartzentruber**[1], **and Karen J. Colley**[2]

From the Department of Biochemistry and Molecular Genetics, University of Illinois at Chicago, College of Medicine, Chicago, Illinois 60607

The polysialyltransferases ST8Sia II and ST8Sia IV polysialylate the glycans of a small subset of mammalian proteins. Their most abundant substrate is the neural cell adhesion molecule (NCAM). An acidic surface patch and a novel α-helix in the first fibronectin type III repeat of NCAM are required for the polysialylation of *N*-glycans on the adjacent immunoglobulin domain. Inspection of ST8Sia IV sequences revealed two conserved polybasic regions that might interact with the NCAM acidic patch or the growing polysialic acid chain. One is the previously identified polysialyltransferase domain (Nakata, D., Zhang, L., and Troy, F. A. (2006) *Glycoconj. J.* 23, 423–436). The second is a 35-amino acid polybasic region that contains seven basic residues and is equidistant from the large sialyl motif in both polysialyltransferases. We replaced these basic residues to evaluate their role in enzyme autopolysialylation and NCAM-specific polysialylation. We found that replacement of Arg^{276}/Arg^{277} or Arg^{265} in the polysialyltransferase domain of ST8Sia IV decreased both NCAM polysialylation and autopolysialylation in parallel, suggesting that these residues are important for catalytic activity. In contrast, replacing Arg^{82}/Arg^{93} in ST8Sia IV with alanine substantially decreased NCAM-specific polysialylation while only partially impacting autopolysialylation, suggesting that these residues may be particularly important for NCAM polysialylation. Two conserved negatively charged residues, Glu^{92} and Asp^{94}, surround Arg^{93}. Replacement of these residues with alanine largely inactivated ST8Sia IV, whereas reversing these residues enhanced enzyme autopolysialylation but significantly reduced NCAM polysialylation. In sum, we have identified selected amino acids in this conserved polysialyltransferase polybasic region that are critical for the protein-specific polysialylation of NCAM.

Polysialic acid is a linear homopolymer of α2,8-linked sialic acid that is added to a small subset of mammalian glycoproteins by the polysialyltransferases (polySTs)[3] ST8Sia II (STX) and ST8Sia IV (PST) (1–4). Substrates for the polySTs include the neural cell adhesion molecule (NCAM) (5, 6), the α-subunit of the voltage-dependent sodium channel (7, 8), CD36, a scavenger receptor found in milk (9), neuropilin-2 expressed by dendritic cells (10), and the polySTs themselves, which can polysialylate their own *N*-glycans in a process called autopolysialylation (11, 12). This small number of polysialylated proteins and other evidence from our laboratory (13–15) suggest that polysialylation is a protein-specific modification that requires an initial protein-protein interaction between the polySTs and their glycoprotein substrates.

The most abundant polysialylated protein is NCAM. The three major NCAM isoforms consist of five Ig domains, two fibronectin type III repeats, and a transmembrane domain and cytoplasmic tail (NCAM140 and NCAM180) or a glycosylphosphatidylinositol anchor (NCAM120) (16). Polysialylation takes place primarily on two *N*-linked glycans in the Ig5 domain (17). We have previously shown that a truncated NCAM140 protein consisting of Ig5, the first fibronectin type III repeat (FN1), the transmembrane region, and cytoplasmic tail is fully polysialylated (13). However, a protein consisting of Ig5, the transmembrane region, and cytoplasmic tail is not polysialylated (13). This suggests that the polySTs recognize and bind the FN1 domain to polysialylate *N*-glycans on the adjacent Ig5 domain. We subsequently identified an acidic patch unique to NCAM FN1, consisting of Asp^{497}, Asp^{511}, Glu^{512}, and Glu^{514} (15).[4] When three of these residues (Asp^{511}, Glu^{512}, and Glu^{514}) are mutated to alanine or arginine, NCAM polysialylation is reduced or abolished, suggesting that the acidic patch is part of a larger recognition region. We anticipate that within this putative recognition region there will be amino acids required for mediating polyST-NCAM binding, and those that do not mediate binding *per se* but instead are required for correct positioning of the enzyme-substrate complex for polysialylation. For example, we have identified a novel α-helix in the FN1 domain that when replaced leads to polysialylation of *O*-glycans found on the FN1 domain rather than *N*-glycans on the Ig5 domain

* This work was supported, in whole or in part, by National Institutes of Health Grant RO1 GM63843 (to K. J. C.).

[S] The on-line version of this article (available at http://www.jbc.org) contains supplemental Fig. 1 and Table 1.

[1] Both authors contributed equally to this work.

[2] To whom correspondence should be addressed: Dept. of Biochemistry and Molecular Genetics, University of Illinois at Chicago, College of Medicine, 900 S. Ashland Ave., M/C 669, Chicago, IL 60607. Tel.: 312-996-7756; Fax: 312-413-0353; E-mail: karenc@uic.edu.

[3] The abbreviations used are: polyST, polysialyltransferase; STX, ST8Sia II or sialyltransferase X; PST, ST8Sia IV or polysialyltransferase-1; NCAM, neural cell adhesion molecule; FN1, first fibronectin type III repeat of NCAM; SML, large sialyl motif; SMS, small sialyl motif; VS, very small sialyl motif; PSTD, polysialyltransferase domain; PBR, polybasic region; DMEM, Dulbecco's modified Eagle's medium; FBS, fetal bovine serum; FITC, fluorescein isothiocyanate; HRP, horseradish peroxidase; PBS, phosphate-buffered saline; Endo N, PK1E endo-*N*-acylneuraminidase; ER, endoplasmic reticulum.

[4] These residues correspond to Asp^{506}, Asp^{520}, Glu^{521}, and Glu^{523} when the sequence numbering includes the 19-amino acid signal sequence and eliminates the 10-amino acid VASE exon included in the protein.

(14). This helix may mediate an interdomain interaction that positions the Ig5 *N*-glycans for polysialylation by an enzyme bound to the FN1 domain (14). Alternatively, the helix could act as a secondary interaction site that positions the polyST properly on the substrate.

The expression of the polySTs is developmentally regulated with high levels of STX and moderate levels of PST expressed throughout the developing embryo (2, 18, 19). STX levels decline after birth, although PST expression persists in specific regions of the adult brain where polysialylated NCAM is involved in neuronal regeneration and synaptic plasticity (18–23). The large size and negative charge of polysialic acid disrupt NCAM-dependent and NCAM-independent interactions, thereby negatively modulating cell adhesion (24–26). Simultaneous disruption of both PST and STX in mice results in severe neuronal defects and death usually within 4 weeks after birth (27). Interestingly, when NCAM expression is also eliminated in these mice, they have a nearly normal phenotype, suggesting the main function of polysialic acid is to modulate NCAM-mediated cell adhesion during development (27). In addition, re-expression of highly polysialylated NCAM has been associated with several cancers, including neuroblastomas, gliomas, small cell lung carcinomas, and Wilms tumor. The presence of polysialic acid is thought to promote cancer cell growth and invasiveness (28–35).

Sialyltransferases, including the polySTs, have three motifs required for catalytic activity (36–38) (see Fig. 1*A*). Sialyl motif Large (SML) is thought to bind the donor substrate CMP-sialic acid (39), whereas sialyl motif Small (SMS) is believed to bind both donor and carbohydrate acceptor substrates (40). The sialyl motif Very Small (SMVS) has a conserved His residue that is required for catalytic activity (38, 41). However, the precise function of this motif is unknown. An additional 4-amino acid motif, motif III, is conserved in the sialyltransferases (42–44). It was suggested that this motif, and particularly His and Tyr residues within its sequence, may be required for optimal activity and acceptor recognition (42).

Angata *et al.* (45) used chimeric enzymes to identify regions within the polySTs required for catalytic activity and NCAM polysialylation. Sequences from PST, STX, and ST8Sia III were used to construct the chimeric proteins. ST8Sia III is an α2,8-sialyltransferase that typically adds one or two sialic acid residues to glycoprotein or glycolipid substrates, can autopolysialylate its own glycans, but cannot polysialylate NCAM (46). Deletion analysis showed that amino acids 62–356 are required for PST catalytic activity. Replacement of segments of this region with corresponding STX or ST8Sia III sequences led to the suggestion that amino acids 62–127 and possibly 194–267 of PST may be required for NCAM recognition (45).

Recently, Troy and co-workers (47, 48) identified a stretch of basic residues, termed the polysialyltransferase domain (PSTD), which is only observed in the two polySTs and not in other sialyltransferases. The PSTD is contiguous with SMS and extends from amino acids 246–277 in PST and 261–292 in STX. Mutation analysis demonstrated that the overall positive charge of this motif is important for activity and identified specific residues required for NCAM polysialylation (Arg^{252}, Ile^{275}, Lys^{276}, and Arg^{277}) (47).

In this study, we have scanned the critical polyST regions identified by the work of Angata *et al.* (45) for sequences that may be involved in protein-protein recognition and NCAM polysialylation. We identified a second polybasic motif that we named the polybasic region (PBR). The PBR is conserved in PST and STX and is located equidistant from the SML of each enzyme. It consists of 35 amino acids of which 7 are the basic amino acids Arg and Lys. We found that the replacement of two specific residues within the PBR (Arg^{82} and Arg^{93} of PST and Arg^{97} and Lys^{108} of STX) have a greater negative effect on NCAM polysialylation than on autopolysialylation. Replacement of acidic residues surrounding PST Arg^{93} led to a similar disparate effect on these processes. Comparison of the critical residues in both the PSTD and PBR demonstrated that the replacement of PSTD residues had an equally negative impact on both NCAM polysialylation and enzyme autopolysialylation, whereas replacement of selected PBR residues more severely impacted NCAM polysialylation, suggesting that the PBR residues may play important roles in NCAM-specific polysialylation.

EXPERIMENTAL PROCEDURES

Tissue culture materials such as Dulbecco's modified Eagle's medium (DMEM), Opti-MEM I, Lipofectin, and fetal bovine serum (FBS) were purchased from Invitrogen. Nitrocellulose membranes were purchased from Schleicher & Schuell. Super-Signal West Pico chemiluminescence reagent was obtained from Pierce. Precision Plus Protein^{TM} standard was obtained from Bio-Rad. Oligonucleotides and anti-V5 tag antibody were purchased from Invitrogen. The QuikChange^{TM} site-directed mutagenesis kit and *Pfu* DNA polymerase were purchased from Stratagene (La Jolla, CA). Human NCAM-Fc cDNA was a gift from Genevieve Rougon (CNRS, Marseilles, France). The cDNA for human ST8Sia IV/PST was obtained from Dr. Minoru Fukuda (Burnham Institute, La Jolla, CA), and the cDNA for human ST8Sia II/STX was obtained from Dr. John Lowe (Genentech, South San Francisco, CA). Protein A-Sepharose was obtained from GE Healthcare. pEndo-N expressing the endo-*N*-acylneuraminidase (endosialidase) cloned from phage PK1E was the kind gift of Dr. Eric Vimr (University of Illinois, Champagne-Urbana). DNA purification kits and nickel-nitrilotriacetic acid-coupled Superflow resin were obtained from Qiagen (Valencia, CA). Protease inhibitors, lysozyme, DNase, and RNase were obtained from Roche Applied Science. Fluorescein isothiocyanate (FITC)-conjugated and horseradish peroxidase (HRP)-conjugated goat anti-mouse antibodies were purchased from Jackson ImmunoResearch. Other chemicals and reagents were obtained from Sigma and Fisher.

Construction of PST and STX Mutants—Mutagenesis was performed using the Stratagene QuikChange^{TM} site-directed mutagenesis kit, according to the manufacturer's protocol. Primers used are listed in supplemental Table 1. Mutations were confirmed by DNA sequencing performed by the DNA Sequencing Facility of the Research Resources Center at University of Illinois at Chicago.

Transfection of COS-1 Cells with NCAM, PST, and STX cDNAs—COS-1 cells maintained in DMEM, 10% FBS were plated on 100-mm tissue culture plates or 12-mm glass cover-

slips and grown at 37 °C, 5% CO_2 until 50–70% confluent. Transfections were performed with Lipofectin according to the Invitrogen protocol. For each plate, cells were co-transfected with PST or STX cDNA, cloned upstream of the epitope tags in the pcDNA3.1 (V5-His B) expression vector, and NCAM-Fc cDNA, cloned in the pIG1 expression vector, at a ratio of 4:1, respectively. To test enzyme autopolysialylation and localization, COS-1 cells plated on coverslips were transfected with 0.5 μg of plasmid DNA mixed with 3 μl of Lipofectin and 300 μl of Opti-MEM I.

Recovery of NCAM-Fc Expressed with PST-V5 or STX-V5 in COS-1 Cells—COS-1 cells were co-transfected with PST-V5 or STX-V5 plasmid DNA and NCAM-Fc plasmid DNA. The transfection mixture was removed 6 h post-transfection, and 4 ml of DMEM, 10% FBS was added to each plate. After an 18-h incubation, cell medium was collected and debris removed by centrifugation. NCAM-Fc consists of the signal sequence and extracellular domains (Ig1-FN2) of a human skeletal muscle isoform of NCAM fused upstream of the Fc region (hinge, CH2, and CH3) of human IgG1. This soluble, secreted NCAM construct was recovered directly from the cell medium by incubation for 2–4 h at 4 °C with 50 μl of protein A-Sepharose beads (50% suspension in phosphate-buffered saline (PBS)), which bind the Fc portion of NCAM-Fc (49). The beads were then washed four times with 1 ml of immunoprecipitation buffer (50 mM Tris, pH 7.5, 150 mM NaCl, 5 mM EDTA, 0.5% Nonidet P-40, 0.1% SDS), followed by one wash with 1 ml of immunoprecipitation buffer containing 1% SDS. Following resuspension in 50 μl of Laemmli sample buffer containing 5% β-mercaptoethanol, samples were heated at 65 °C for 10 min and separated on a SDS-polyacrylamide gel (3% stacking gel, 5% separating gel). To evaluate relative enzyme expression levels, cells were lysed in 1 ml of immunoprecipitation buffer, and an aliquot was mixed with an equal volume of Laemmli sample buffer containing 5% β-mercaptoethanol, boiled at 110 °C for 10 min, and resolved on a SDS-polyacrylamide gel (5% stacking gel, 7.5% separating gel).

Immunoblot Analysis of Polysialylation and Protein Expression Levels—Following SDS-PAGE, proteins were transferred to a nitrocellulose membrane for 18 h at 500 mA. Following a 1-h blocking step in 5% nonfat dry milk in Tris-buffered saline, pH 8.0, 0.1% Tween 20 (blocking buffer), membranes were incubated with primary and HRP-conjugated secondary antibodies prior to development. To detect polysialic acid, membranes were incubated overnight with a 1:50–1:250 dilution of OL.28 anti-polysialic acid antibody in 2% nonfat dry milk in Tris-buffered saline, pH 8.0, and for 1 h with HRP-conjugated goat anti-mouse IgM diluted 1:4000 in blocking buffer. For analysis of enzyme expression, membranes were incubated for 2 h with an anti-V5 tag antibody diluted 1:5000 in blocking buffer and HRP-conjugated goat anti-mouse IgG diluted 1:4000 in blocking buffer. Following primary antibody incubation, blots were washed two times for 15 min with Tris-buffered saline, pH 8.0, 0.1% Tween 20. Following the secondary antibody incubation, blots were washed four times for 15 min with Tris-buffered saline, pH 8.0, 0.1% Tween 20. Immunoblots were developed using the SuperSignal West Pico chemiluminescence kit (Pierce) and Kodak Bio-Max MR film.

Immunofluorescence Analysis of Enzyme Localization and Activity—COS-1 cells were transfected with PST or STX plasmid DNA, as described above. One milliliter of DMEM, 10% FBS was added to the transfection mixture 6 h post-transfection. After an 18-h incubation, cells were washed twice with 1 ml of PBS and permeabilized with −20 °C methanol to visualize both internal structures and the cell surface. To detect enzymes, cells were incubated with a 1:250 dilution of the anti-V5 tag antibody, followed by incubation with FITC-conjugated goat anti-mouse IgG diluted 1:100 in immunofluorescence blocking buffer (5% normal goat serum in PBS). To evaluate autopolysialylation and catalytic activity, cells were incubated with a 1:100 dilution of OL.28 anti-polysialic acid antibody, followed by incubation with FITC-conjugated goat anti-mouse IgM diluted 1:100 in immunofluorescence blocking buffer. Following each antibody step, coverslips were washed four times for 5 min with 1 ml of PBS. Coverslips were mounted on glass slides using mounting medium (15% (w/v) Vinol 205 polyvinyl alcohol, 33% (w/v) glycerol, 0.1% azide in PBS, pH 8.5). Cells were visualized using a Nikon Axiophot microscope equipped with epifluorescence illumination and either a 40× FLUOR Ph3DL objective or 60× oil immersion Plan Apochromat objective. Pictures were taken using a SPOT RT color digital camera and processed using Spot RT software version 3.5.1 (Diagnostic Instruments Inc, Sterling Heights, MI).

Quantification of Autopolysialylation and NCAM Polysialylation by Pulse-Chase Analysis and Densitometry—To evaluate autopolysialylation, PST-V5 and its mutants were transiently expressed in COS-1 cells. Eighteen hours post-transfection, cells were incubated with 5 ml of Met/Cys-free DMEM for 1 h. Cells were then labeled for 1 h in 4 ml of fresh Met/Cys-free DMEM containing 100 μCi/ml ^{35}S-Express protein labeling mix (PerkinElmer Life Sciences). The labeling media was then removed; cells were washed with 10 ml of PBS, and 4 ml of fresh DMEM, 10% FBS was added for an additional 3 h. Following the 3-h chase, the media were recovered, centrifuged to remove debris, and frozen at −20 °C. Cleaved and secreted polyST proteins were immunoprecipitated from cell media using 6 μl of anti-V5 tag antibody and 75 μl of protein A-Sepharose beads (50% suspension in PBS). To evaluate NCAM polysialylation by PST and its mutants, COS-1 cells transiently co-expressing a wild type or mutant PST protein and NCAM-Fc (PST cDNA:NCAM-Fc cDNA = 4:1) were labeled with ^{35}S-Express protein labeling mix as described above, and NCAM-Fc was recovered from the cell medium by incubation with 75 μl of protein A-Sepharose beads for 2–4 h at 4 °C. Immunoprecipitation beads were washed, resuspended in 75 μl of Laemmli sample buffer containing 5% β-mercaptoethanol, and heated at 65 °C for 10 min. Samples were separated on either 5% (NCAM-Fc) or 7.5% (polySTs) SDS-polyacrylamide gels. Radiolabeled proteins were visualized by fluorography using 10% 2,5-diphenyloxazole in dimethyl sulfoxide (50), and gels were exposed to Kodak BioMax MR film. For each sample, the amount of polyST protein expressed was assessed by immunoblotting using the anti-V5 epitope tag, as described above. To quantify levels of polyST autopolysialylation and NCAM-Fc polysialylation, densitometry analysis was performed using a Bio-Rad Chemidoc XRS system and the Bio-Rad Quantity One 4.6.2

A. Schematic representation of PST and STX

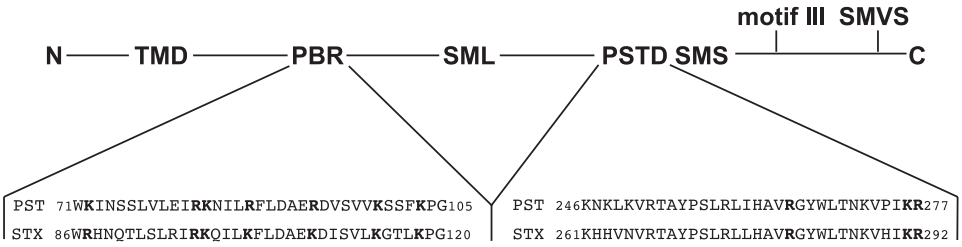

B. PSTD mutants of PST

K276A/R277A	246KNKLKVRTAYPSLRLIHAVRGYWLTNKVPI**AA**277
K276Q/R277I	246KNKLKVRTAYPSLRLIHAVRGYWLTNKVPI**QI**277
R265A	246KNKLKVRTAYPSLRLIHAV**A**GYWLTNKVPIKR277
R265A/K276A/R277A	246KNKLKVRTAYPSLRLIHAV**A**GYWLTNKVPI**AA**277

C. PBR mutants of PST and STX

PST K72A	71W**A**INSSLVLEIRKNILRFLDAERDVSVVKSSFKPG105
PST R82A	71WKINSSLVLEI**A**KNILRFLDAERDVSVVKSSFKPG105
PST K83A	71WKINSSLVLEIR**A**NILRFLDAERDVSVVKSSFKPG105
PST R87A	71WKINSSLVLEIRKNIL**A**FLDAERDVSVVKSSFKPG105
PST R93A	71WKINSSLVLEIRKNILRFLDAE**A**DVSVVKSSFKPG105
PST K99A	71WKINSSLVLEIRKNILRFLDAERDVSVV**A**SSFKPG105
PST K103A	71WKINSSLVLEIRKNILRFLDAERDVSVVKSSF**A**PG105
PST R82A/R93A	71WKINSSLVLEI**A**KNILRFLDAE**A**DVSVVKSSFKPG105
PST R82K/R93K	71WKINSSLVLEI**K**KNILRFLDAE**K**DVSVVKSSFKPG105
PST R82D/R93D	71WKINSSLVLEI**D**KNILRFLDAE**D**DVSVVKSSFKPG105
PST E92A/D94A	71WKINSSLVLEIRKNILRFLDA**A**R**A**VSVVKSSFKPG105
PST E92D/D94E	71WKINSSLVLEIRKNILRFLDA**DRE**VSVVKSSFKPG105
STX R97A	86WRHNQTLSLRI**A**KQILKFLDAEKDISVLKGTLKPG120
STX K108A	86WRHNQTLSLRIRKQILKFLDAE**A**DISVLKGTLKPG120
STX R97A/K108A	86WRHNQTLSLRI**A**KQILKFLDAE**A**DISVLKGTLKPG120
STX R97K/K108R	86WRHNQTLSLRI**K**KQILKFLDAE**R**DISVLKGTLKPG120

FIGURE 1. **PST and STX polybasic regions and mutants generated for this study.** *A*, representation of the polySTs and their polybasic regions and sialyl motifs. The PBR is a 35-amino acid region present in both PST and STX, equidistant from the SML of each enzyme and rich in conserved positively charged amino acids. The PSTD is a region identified by Nakata *et al.* (47) that is 32 amino acids in length, rich in basic residues, and contiguous with the SMS of the enzymes. The sialyl motifs (SML, SMS, SMVS, and motif III) are regions of homology found in all sialyltransferases that are believed to be involved in substrate and donor interactions. *B*, PSTD of PST and the mutants made in this region that are used in this study. *C*, PBR of PST and STX and the mutants made in this region that are used in this study.

program. Densitometric results for each sample were normalized for protein expression, and all results were compared with those for PST (PST autopolysialylation and NCAM-Fc polysialylation levels set to 100%).

PK1E Endo-N-acylneuraminidase N (Endo N) Purification and Sample Treatment—All reagents, cells, and protocols for expression and purification of Endo N were kindly provided by Dr. Eric Vimr, University of Illinois. The pEndo-N expression plasmid consists of the full-length gene of the Endo N tail spike protein from the phage K1E cloned into pQE60 that fuses a carboxyl-terminal His_6 tag to the protein (Qiagen). The expression of PK1E Endo N was induced with 1 mM isopropyl 1-thio-β-D-galactopyranoside (final concentration) for 3 h at 37 °C in an M15 bacterial strain harboring both pEndo-N-QE60 and pRep4 plasmids (51). The soluble enzyme was then purified by nickel affinity chromatography according to the method provided by Qiagen. PK1E Endo N requires an α2,8-sialic acid chain of ~8 units for cleavage and is therefore expected to leave a short (~4 unit) α2, 8-sialic acid chain at the terminus of the glycan it has cleaved (52). The polysialic acid chains on metabolically labeled, immunoprecipitated PST were digested on the protein A-Sepharose beads by incubation with a 1:10 dilution of Endo N (30 μg/ml) in 20 mM Tris-HCl, pH 7.4, for 2 h at 37 °C.

RESULTS

Our previous work demonstrated that NCAM FN1 was required for the polysialylation of *N*-glycans on the adjacent Ig5 domain and that an acidic surface patch and a unique α-helix in FN1 played a role in this process (13–15). We hypothesize that NCAM-specific polysialylation involves protein-protein interactions between NCAM FN1 and the polySTs. These protein interactions would position a polyST to polysialylate the *N*-glycans on the Ig5 domain and also potentially allow stable binding to promote the polymerization of the polysialic acid chains. Alternatively or in addition, after their recognition of substrate via a protein-protein interaction, the polySTs may bind directly to the growing polysialic acid chain to promote polymerization, as suggested by Nakata *et al.* (47). In an effort to identify residues in the polySTs that may be required for NCAM-specific polysialylation, we evaluated the polyST sequences for regions rich in basic residues that could interact with the FN1 acidic patch and even polysialic acid itself. In this work we evaluate a polybasic region previously identified by Nakata *et al.* (47), the PSTD, as well as a new polybasic region found within a stretch of amino acids (62–127 of PST) that the earlier work of Angata *et al.* (45) had suggested is critical for NCAM-specific polysialylation. This 35-amino acid region, which we call the PBR, is located equidistant from the SML of each enzyme. It spans amino acids 71–105 in PST and amino acids 86–120 in STX. A schematic representation of the polySTs, including the relative positions of the PBR and PSTD and their sequences, is shown in Fig. 1*A*. In this study we compare the role of these two polyST polybasic regions in general catalytic activity, as measured by enzyme autopolysialylation, and in NCAM-specific polysialylation. Our goal was to find

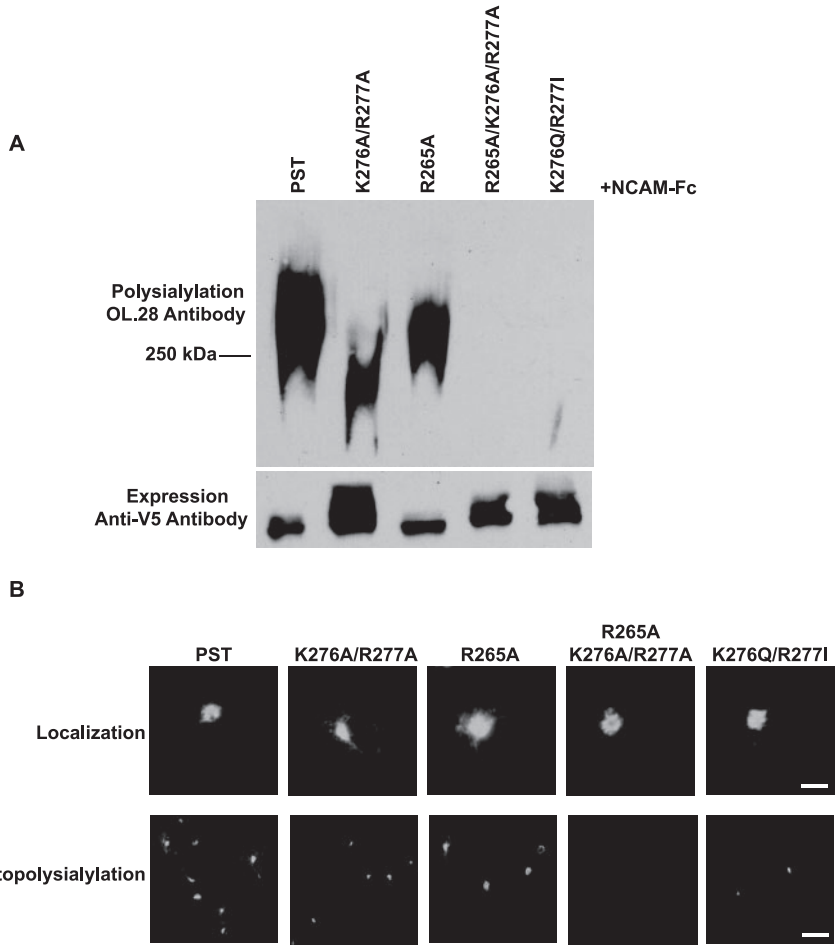

FIGURE 2. **Mutations in Arg^{265}, Lys^{276}, and Arg^{277} in the PSTD of PST substantially decrease its ability to both autopolysialylate and polysialylate NCAM without altering Golgi localization.** COS-1 cells were transiently co-transfected with NCAM-Fc and wild type PST-V5 or PST-V5 containing mutations in Arg^{265} (R265A), Lys^{276}, and Arg^{277} (K276A/R277A or K276Q/R277I) or all three residues (R265A/K276A/R277A). *A, top panel,* polysialylation of NCAM-Fc by wild type PST and the PST PSTD mutants was measured by immunoblotting with OL.28 anti-polysialic acid antibody (*Polysialylation, OL.28 Antibody*). *Bottom panel,* to assess the expression levels of the PST proteins, an aliquot of cell lysate was boiled to remove polysialic acid and immunoblotted with the anti-V5 tag antibody (*Expression, Anti-V5 Antibody*). *B, top panels,* COS-1 cells transiently expressing PST and PST PSTD mutants K276A/R277A, R265A, R265A/K276A/R277A, and K276Q/R277I were analyzed by indirect immunofluorescence microscopy using the anti-V5 tag antibody to assess protein localization (*Localization*). *Bar,* 10 μm. *Bottom panels,* COS-1 cells transiently expressing PST and PST PSTD mutants K276A/R277A, R265A, R265A/K276A/R277A, and K276Q/R277I were analyzed by indirect immunofluorescence microscopy using OL.28 anti-polysialic acid antibody to assess autopolysialylation (*Autopolysialylation*). *Bar,* 50 μm.

sequences that when replaced would decrease or eliminate NCAM polysialylation without disrupting enzyme autopolysialylation, with the rationale that this would allow us to identify amino acids that could be involved in the predicted polyST-NCAM interaction.

Role of PSTD Residues Arg^{265}, Lys^{276}, and Arg^{277} in PST Catalytic Activity and NCAM Polysialylation—Using site-directed mutagenesis and an *in vitro* activity assay, Nakata *et al.* (47) concluded that the overall positive charge of the PSTD, and specifically Arg^{252}, Ile^{275}, Lys^{276}, and Arg^{277}, are essential for NCAM polysialylation. They demonstrated that a double mutant of PST, in which Lys^{276} is replaced by glutamine and Arg^{277} is replaced by isoleucine (K276Q/R277I or KR (47)), exhibited a substantially decreased ability to polysialylate NCAM. Here we use our cellular assays to evaluate the activity of this mutant and others in the PSTD to compare the relative contributions of these PSTD residues to NCAM polysialylation.

For our study we have evaluated the PST K276Q/R277I mutant described above and a similar mutant, K276A/R277A, in which we replaced these PST residues with alanine (Fig. 1*B*, *K276Q/R277I* and *K276A/R277A*). We have also replaced Arg^{265} in the PSTD with alanine (Fig. 1*B*, *R265A*). This residue is found in both polySTs but was not analyzed by Nakata *et al.* (47). Following co-expression of the wild type and mutant PST proteins with soluble NCAM-Fc in COS-1 cells, polysialylation of the NCAM-Fc protein was evaluated by OL.28 immunoblotting as described under "Experimental Procedures." We found that PST R265A and PST K276A/R277A exhibited reduced abilities to polysialylate NCAM-Fc, as indicated by a decrease in anti-polysialic acid antibody reactivity and/or a decrease in the molecular mass of the modified NCAM-Fc protein. Strikingly, PST K276Q/R277I and PST R265A/K276A/R277A were unable to detectably polysialylate NCAM-Fc (Fig. 2*A*, *top panel*). Decreased expression levels of the various mutants could not explain the observed decreases in NCAM-Fc polysialylation because R265A was expressed at a similar level as wild type PST and the other three mutants appeared to be expressed at higher levels than wild type PST (Fig. 2*A*, *bottom panel*).

The polySTs are predominantly Golgi enzymes that are found in part on the cell surface and as cleaved, soluble forms in the cell media when overexpressed (11, 49, 53). These enzymes are also capable of polysialylating their own *N*-glycans (autopolysialylation), and this can be examined by expressing the polySTs in COS-1 cells that contain no other polyST substrates and staining these cells with the OL.28 anti-polysialic acid antibody (11, 49, 53). To determine whether the decreased ability of these PST PSTD mutants to polysialylate NCAM reflects their misfolding and ER retention and/or a general decrease in catalytic activity, we evaluated their subcellular localization and autopolysialylation by immunofluorescence microscopy. Using the anti-V5 tag antibody, we found that the four PSTD mutants exhibited tight perinuclear Golgi staining like wild type PST. These proteins also exhibited variable amounts of diffuse staining surrounding the perinu-

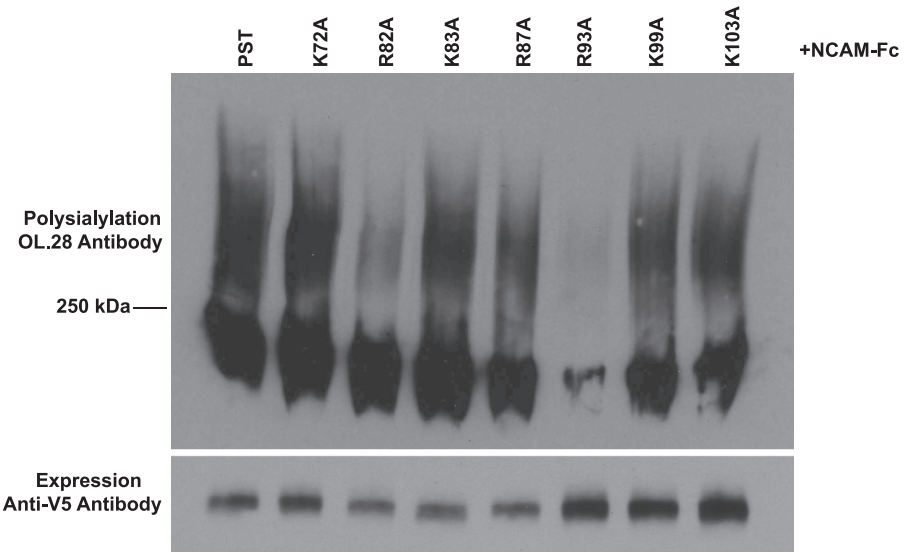

FIGURE 3. **Ability of PST to polysialylate NCAM is decreased by replacement of specific PBR basic residues.** COS-1 cells were transiently co-transfected with NCAM-Fc and wild type PST-V5 or PST-V5 containing single arginine or lysine to alanine mutations. *Top panel,* NCAM-Fc was recovered from the cell media using protein A-Sepharose and polysialylation measured by immunoblotting with OL.28 anti-polysialic acid antibody (*Polysialylation, OL.28 Antibody*). *Bottom panel,* to assess the expression levels of the PST proteins, an aliquot of cell lysate was boiled to remove polysialic acid and immunoblotted with the anti-V5 tag antibody (*Expression, Anti-V5 Antibody*).

clear Golgi region suggestive of ER staining, and likely reflecting protein overexpression in the COS-1 cell system (Fig. 2*B*, *Localization*). Using the OL.28 anti-polysialic acid antibody, we found that all four PSTD mutants differed from wild type PST in their ability to autopolysialylate (Fig. 2*B*, *Autopolysialylation*). Autopolysialylated polySTs have been detected both in the perinuclear Golgi region and at the cell surface (clearly delineating the cell borders) (11). The PST R265A/K276A/R277A mutant exhibited no detectable autopolysialylation; the K276Q/R277I mutant showed little detectable autopolysialylation, and the K276A/R277A and R265A mutants were intermediate in their ability to autopolysialylate. In sum, the intrinsic catalytic activities of PSTD mutants, as measured by autopolysialylation, largely reflected their ability to polysialylate NCAM-Fc. These results suggest that the changes made to these PSTD amino acids may impact the general catalytic activity of the enzyme.

Amino Acid Residues within the PBR Are Required for Efficient NCAM Polysialylation—To evaluate the role of the PST PBR in NCAM polysialylation, all seven basic residues in this region were individually replaced with alanine (Fig. 1*C*). These mutants were co-expressed with NCAM-Fc, and polysialylation of this soluble NCAM protein was measured by immunoblotting with the anti-polysialic acid antibody, OL.28. The PST mutants K72A, K83A, R87A, K99A, and K103A polysialylated NCAM-Fc at levels similar to wild type PST (Fig. 3, *top panel*). However, PST R82A and PST R93A exhibited a significantly reduced ability to polysialylate NCAM-Fc (Fig. 3, *top panel*). Analysis of relative expression levels of wild type PST and its PBR mutants demonstrated that these proteins were expressed at comparable levels, and indicated the reduced NCAM-Fc polysialylation by PST R82A and PST R93A was not because of their decreased expression (Fig. 3, *bottom panel*).

Charge of PST Arg^{82} and Arg^{93} Is Critical for NCAM Polysialylation—Replacement of PST Arg^{82} or Arg^{93} reduced polysialylation of NCAM-Fc but did not eliminate it. However, we found that a PST R82A/R93A double mutant was unable to polysialylate NCAM-Fc (Fig. 4*A*). To determine whether the specific amino acid or its charge is critical for NCAM polysialylation, we replaced Arg^{82} and Arg^{93} with lysine residues to generate R82K/R93K (Fig. 1*C*). Interestingly, although replacement of these specific basic amino acids with neutral alanine residues dramatically reduced or eliminated NCAM polysialylation, replacement with the alternative positively charged amino acid seemed to have little effect on the ability of the enzyme to polysialylate NCAM-Fc (Fig. 4*A*, *R82A/R93A versus R82K/R93K*).

PST PBR Mutations That Eliminate NCAM Polysialylation Do Not Alter Enzyme Autopolysialylation or Golgi Localization—To determine whether these mutations in PST decrease or eliminate NCAM polysialylation because they lead to misfolding and ER retention, or because they generally inactivate the enzymes, we localized these proteins and determined their ability to autopolysialylate using immunofluorescence microscopy (Fig. 4*B*). Following expression in COS-1 cells, we found that the PST R82A, R93A, R82A/R93A, and R82K/R93K mutants, were localized predominantly in the Golgi, like wild type PST, indicating these enzymes were not grossly misfolded and exited the ER efficiently (Fig. 4*B*, *Localization*). More importantly, staining expressing cells with the OL.28 antibody demonstrated that the mutant enzymes were catalytically active as shown by their ability to autopolysialylate (Fig. 4*B*, *Autopolysialylation*). In other experiments, we also tested the polysialylation of membrane-bound NCAM by the PST PBR mutants. PST R82A/R93A demonstrated a significantly reduced ability to polysialylate NCAM140, whereas PST R82K/R93K could polysialylate NCAM140 as efficiently as the wild type enzyme (data not shown). In sum, the decreased polysialylation of NCAM by PST R82A, R93A, and R82A/R93A is not because of gross misfolding and ER retention or the general inactivity of the mutant proteins.

STX PBR Mutations Have a Similar Effect on NCAM Polysialylation as the Analogous PST PBR Mutants—Analyses of the analogous amino acids in the PBR of STX (Arg^{97} and Lys^{108}) yielded similar results. We found that the STX R97A/K108A mutant localized to the Golgi and was autopolysialylated (appeared somewhat reduced) but was unable to polysialylate NCAM-Fc (supplemental Fig. 1, *A* and *B*, *R97A/K108A*). Replacing these residues with the alternative positively charged amino acids in an STX R97K/K108R mutant led to the recovery of NCAM-Fc polysialylation (supplemental Fig. 1, *A* and *B*,

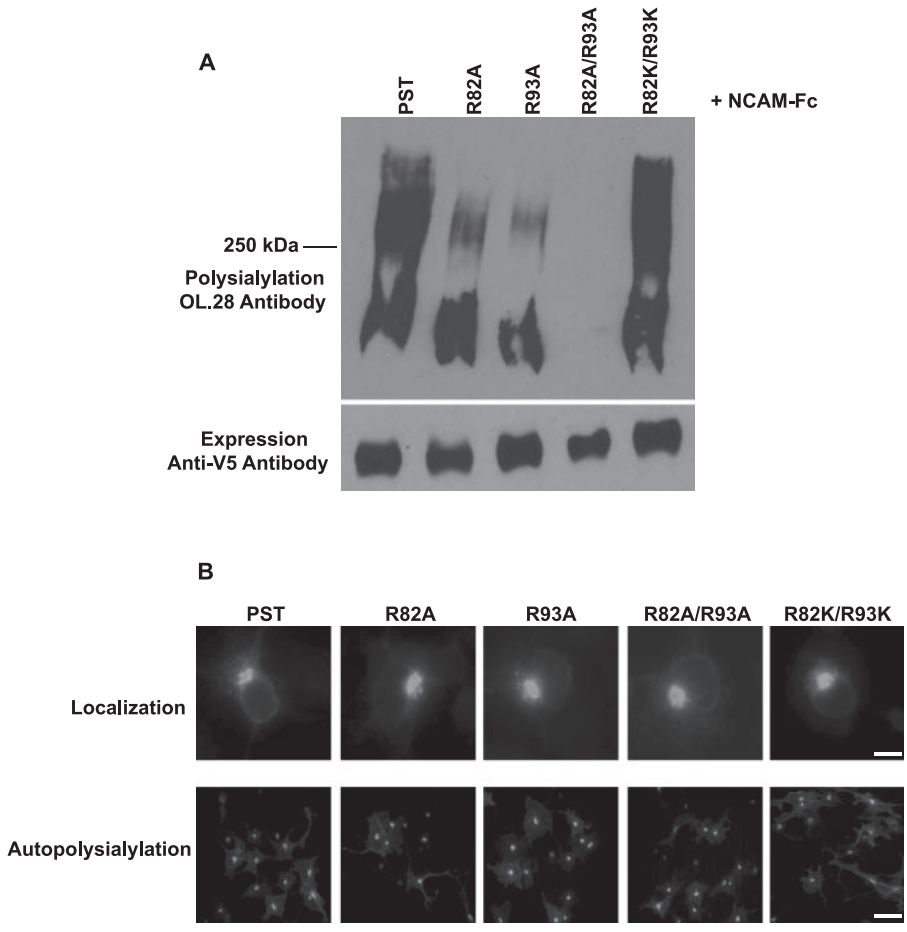

FIGURE 4. **Analysis of the localization, autopolysialylation, and NCAM polysialylation of PST PBR Arg^{82} and Arg^{93} single and double mutants.** *A,* polysialylation of NCAM-Fc by PST, PST R82A, PST R93A, PST R82A/R93A, and PST R82K/R93K was compared by immunoblotting with the OL.28 anti-polysialic acid antibody following expression in COS-1 cells (*top panel*). PolyST protein expression was assessed by immunoblotting with the anti-V5 epitope tag antibody (*bottom panel*). *B,* COS-1 cells transiently expressing wild type or mutant PST-V5 were fixed with methanol to visualize internal structures and the cell surface, and analyzed by indirect immunofluorescence microscopy for enzyme localization (*Localization, bar,* 10 μm) and autopolysialylation (*Autopolysialylation*, *bar,* 50 μm).

R97K/K108R). These results taken together with those in Fig. 4 suggest that the positive charge of specific basic amino acids within the PBR of both PST and STX are required for NCAM-specific polysialylation.

Residues Surrounding PST Arg^{93} Are Also Required for NCAM Polysialylation—Our data suggest that the positive charges of PST Arg^{82} and Arg^{93} and STX Arg^{97} and Lys^{108} are important for NCAM-specific polysialylation. Consequently, it was surprising to find that PST Arg^{93} and STX Lys^{108} are both flanked by negatively charged glutamate and aspartate residues (PST Glu^{92}-Arg^{93}-Asp^{94} and STX Glu^{107}-Lys^{108}-Asp^{109}). Notably, these residues are conserved only in the two polySTs and are not found in other ST8Sia enzymes (Fig. 8). We wondered whether replacing Glu^{92} and Asp^{94} with alanine would impact the ability of the enzyme to polysialylate NCAM and even enhance that ability by increasing the overall positive charge of the region. Unexpectedly, we found that the PST E92A/D94A mutant was not able to detectably polysialylate NCAM-Fc and demonstrated substantially reduced autopolysialylation even though it was transported out of the ER efficiently and localized in the Golgi (Fig. 5, *A* and *B*). To determine whether the charge of these two residues was again the critical factor, we replaced Glu^{92} with aspartate and Asp^{94} with glutamate. This PST E92D/D94E mutant was localized properly and appeared to possess an enhanced autopolysialylation ability (Fig. 5*B*) but exhibited a substantially reduced ability to polysialylate NCAM-Fc (Fig. 5*A*). In sum, these data suggest that residues Glu^{92}-Arg^{93}-Asp^{94} in PST are critical for NCAM-specific polysialylation. Although residue 93 must be positively charged (either Arg or Lys), residues 92 and 94 must be Glu and Asp, respectively, to allow the protein-specific polysialylation of NCAM.

Quantitative Comparison of the Changes in Enzyme Autopolysialylation and NCAM Polysialylation by PST with Mutations in the PSTD and PBR—The immunoblotting and immunofluorescence microscopy results described above suggested that the PST PBR mutations, R82A/R93A and E92D/D94E, negatively affected NCAM polysialylation more than they did autopolysialylation, whereas the PST PSTD mutants seemed to affect both processes similarly. To quantitatively compare the abilities of the PST PBR and PSTD mutants to autopolysialylate and polysialylate NCAM, we used pulse-chase analysis and densitometry. Here we chose to evaluate only those PST mutants that exhibited compromised NCAM polysialylation and/or autopolysialylation in our immunoblotting and immunofluorescence assays in Figs. 2, 4, and 5. COS-1 cells expressing a PST protein alone or co-expressing a PST protein with NCAM-Fc were labeled with ^{35}S-Express label for 1 h and chased for 3 h. Autopolysialylated PST proteins were immunoprecipitated from cell media using the anti-V5 epitope tag antibody and protein A-Sepharose, whereas NCAM-Fc was recovered from cell media using protein A-Sepharose. Following separation on SDS-polyacrylamide gels, radiolabeled bands were visualized by fluorography and quantified by densitometry. To normalize the data, the expression of each PST protein was determined by immunoblotting, following removal of polysialic acid by boiling.

We first evaluated the autopolysialylation of the PST mutants (Fig. 6). To define the migration of autopolysialylated PST on the SDS gel, we used bacteriophage PK1E endo-*N*-acylneuraminidase (Endo N), an enzyme that specifically removes α2,8-polysialic acid and requires a chain of ~8 units or longer for activity (52). Autopolysialylated PST migrated with a molecular mass between ~75 and 250 kDa and collapsed to a broad 48–65-kDa band when the immunoprecipitated protein was

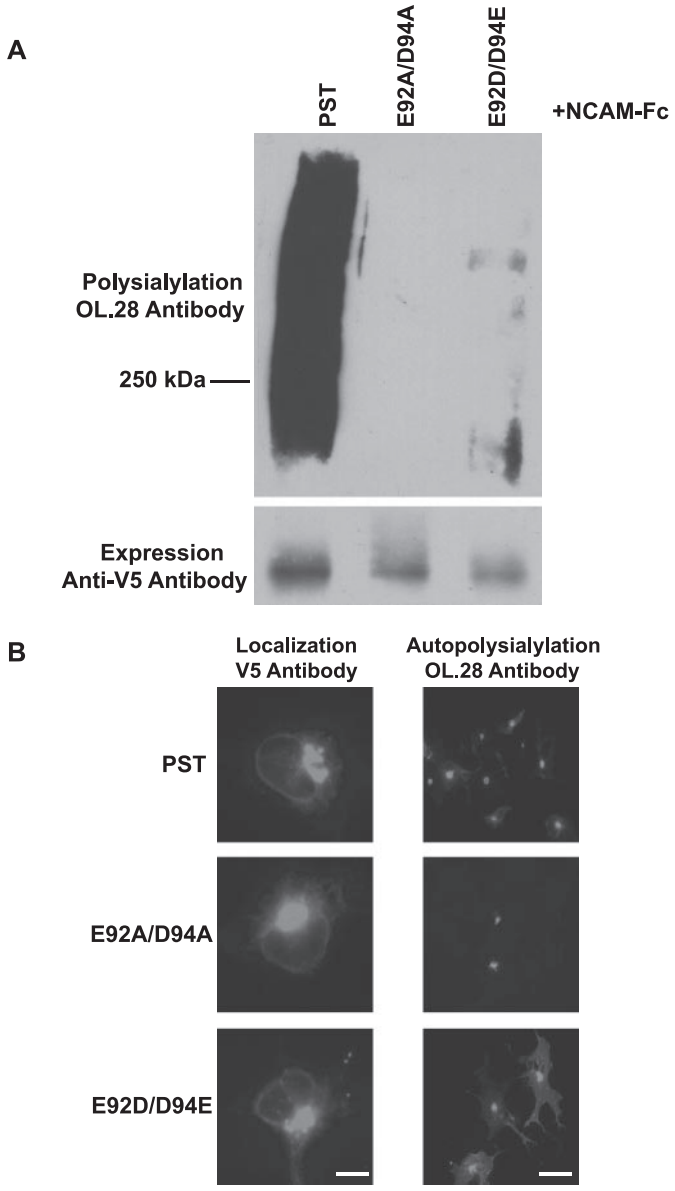

FIGURE 5. **Glu[92] and Asp[94] in the PBR of PST are critical for NCAM polysialylation.** *A*, polysialylation of NCAM-Fc by co-expressed PST, PST E92A/D94A, and PST E92D/D94E was compared using OL.28 immunoblotting (*top panel*). Relative enzyme expression levels were determined by anti-V5 tag antibody immunoblotting of aliquots of cell lysates (*bottom panel*). *B*, localization (*Localization, V5 Antibody*, *bar,* 10 μm) and autopolysialylation (*Autopolysialylation, OL.28 Antibody*, *bar,* 50 μm) of PST, PST E92A/D94A, and PST E92D/D94E was determined by immunofluorescence microscopy.

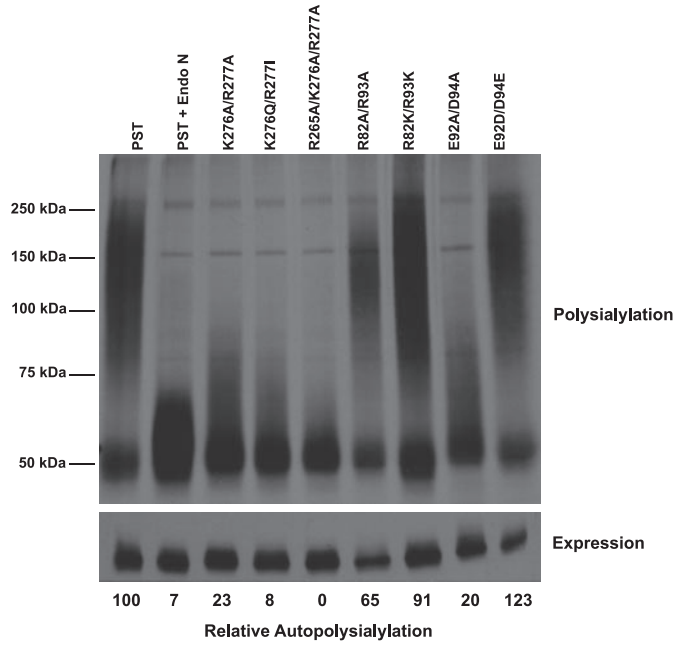

FIGURE 6. **Metabolic labeling reveals different patterns of autopolysialylation for PST with mutations in the PBR and PSTD.** *Top panel,* PST-V5 and selected PBR and PSTD mutants were transiently expressed in COS-1 cells. Expressing cells were metabolically labeled with ^{35}S-Met/Cys for 1 h and chased with unlabeled media for 3 h. Proteins were recovered from cell media using the anti-V5 tag antibody and analyzed by SDS-PAGE and fluorography. Digestion of autopolysialylated PST with Endo N (*PST + Endo N*) demonstrates that autopolysialylated PST proteins migrate between ~75 and 250 kDa. *Bottom panel,* relative polyST protein expression was determined by immunoblot analysis using the anti-V5 epitope tag antibody. Densitometry analysis was used to quantify the autopolysialylation of each polyST protein and its protein expression. These numbers were used to compare the autopolysialylation of each PST mutant to that of wild type PST (set at 100%). These values are indicated as *Relative Autopolysialylation*.

treated with Endo N (Fig. 6, *PST* and *PST + Endo N*). The broadness of the Endo N-treated PST band is likely a result of short (~4 units) oligosialic acid chains remaining on the *N*-glycans of PST (52).

This analysis revealed three distinct groups of PST proteins with respect to their ability to autopolysialylate. The first group was composed of those enzymes that were autopolysialylated like wild type PST and migrated as broad bands of 75–250 kDa. This group included the PBR mutants R82A/R93A, R82K/R93K, and E92D/D94E. The proportion of each mutant protein autopolysialylated varied with R82A/R93A at 65%, R82K/R93K at 91%, and E92D/D94E at 123% of the wild type PST autopolysialylation level. The extent of autopolysialylation by these mutants as measured by the pulse-chase analysis correlated well with the numbers of cells stained and the intensity of staining in our OL.28 immunofluorescence microscopy analysis of autopolysialylation in Figs. 4 and 5 (E92D/D94E > PST = R82K/R93K > R82A/R93A). The second group was composed of those enzymes that were clearly modified, possibly with shorter or fewer sialic acid chains, and migrated as lower molecular mass bands between ~65 and 90 kDa. This group included the PSTD mutants K276A/R277A and K276Q/R277I and the PBR mutant E92A/D94A. Only small proportions of these proteins were autopolysialylated using the 75–250-kDa window in the densitometry analysis (K276A/R277A, 23%; K276Q/R277I, 8%; E92A/D94A, 20%) (Fig. 6). Again, this analysis in general correlated with the OL.28 staining of cells expressing these mutants in Figs. 2 and 5. The last group contained only one member, the PSTD mutant R265A/K276A/R277A, which did not appear to be polysialylated in either the pulse-chase analysis or the OL.28 immunofluorescence microscopy assay (Figs. 2 and 6).

Next we evaluated the ability of these mutants to polysialylate NCAM using the pulse-chase analysis described above (Fig. 7*A*, *top panel*). For the PST PSTD mutants, decreases in NCAM polysialylation closely mirrored decreases in autopolysialylation ability (see comparison in Fig. 7*B*). The K276A/R277A protein exhibited reduced autopolysialylation (23%) and NCAM polysialylation (30%), as did the K276Q/R277I protein (8%

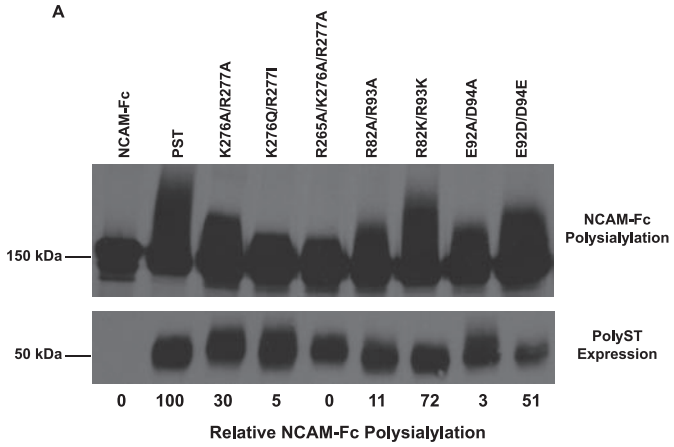

B

PolyST	Relative Autopolysialylation	Relative NCAM-Fc Polysialylation	
		Pulse-Chase	Immunoblot
PST	100%	100%	100%
K276A/R277A	23%	30%	21%
K276Q/R277I	8%	5%	0%
R265A/K276A/R277A	0%	0%	0%
R82A/R93A	65%	11%	0%
R82K/R93K	91%	72%	90%
E92A/D94A	20%	3%	0%
E92D/D94E	123%	51%	7%

FIGURE 7. **Metabolic labeling reveals different patterns of NCAM-Fc polysialylation for PST with mutations in the PBR and PSTD.** *A, top panel,* PST-V5 and selected PBR and PSTD mutants were transiently co-expressed with NCAM-Fc in COS-1 cells. Expressing cells were metabolically labeled with ^{35}S-Met/Cys for 1 h and chased with unlabeled media for 3 h. Radiolabeled NCAM-Fc was recovered from cell media using protein A-Sepharose and analyzed by SDS-PAGE and fluorography. Polysialylated NCAM-Fc was defined as those molecules migrating with molecular masses greater than unpolysialylated NCAM-Fc (*NCAM-Fc*). *Bottom panel*, relative polyST protein expression was determined by immunoblot analysis using the anti-V5 epitope tag antibody. Densitometry analysis was used to quantify the polysialylation of NCAM-Fc by each polyST protein and polyST protein expression. These numbers were used to compare NCAM-Fc polysialylation by each PST mutant to that of wild type PST (set at 100%). These values are indicated as *Relative NCAM-Fc Polysialylation*. *B*, comparison of *Relative Autopolysialylation* and *NCAM-Fc Polysialylation* (pulse-chase numbers are from *A*, and immunoblot numbers are averages of two experiments) for PST and its mutants.

autopolysialylation and 5% NCAM polysialylation), whereas the R265A/K276A/R277A protein was inactive in both processes (Figs. 6 and 7). Densitometric scanning of the lanes of the representative OL.28 immunoblots provided similar results in most cases (Fig. 7*B*).

Our quantitative evaluation of the PST PBR mutants demonstrated that for some, changes in NCAM polysialylation did not always mirror changes in autopolysialylation, largely in accord with our OL.28 immunoblot and immunofluorescence analyses in Figs. 4 and 5. Replacement of Arg^{82} and Arg^{93} with alanine disproportionately decreased NCAM polysialylation to 11% that of wild type PST and only decreased autopolysialylation to 65% that of the unaltered enzyme (Figs. 6 and 7). The inability of OL.28 to recognize the NCAM modified by the R82A/R93A mutant in the immunoblot analysis suggests that the modification detected by the pulse-chase analysis could be due in part to multiple, shorter sialic acid chains less than 5 units in length that are not recognized by the OL.28 antibody (54). Replacement of these residues with lysines allowed recovery of both NCAM polysialylation (72%) and autopolysialylation (91%), although the OL.28 reactivity on immunoblot suggests that more OL.28-reactive polysialic acid chains were added to the NCAM modified by the R82K/R93K mutant than suggested by the quantification of the pulse-chase labeling data (compare R82K/R93K in Figs. 4 and Fig. 7).

Replacement of Glu^{92} and Asp^{94} with alanine largely inactivated the enzyme for NCAM polysialylation (3%), with some residual auto-modification observed by pulse-chase analysis (20%). Interestingly, pulse-chase analysis indicated that switching these residues in the E92D/D94E mutant enhanced autopolysialylation (123%) but significantly decreased NCAM polysialylation (51%). The OL.28 immunoblotting shown in Fig. 5 suggested a more substantial decrease in NCAM-Fc polysialylation by the E92D/D94E mutant (a decrease to 7% rather than 51% of the wild type PST level). Because the molecular mass of the E92D/D94E-modified NCAM-Fc is lower than that modified by R82K/R93K or wild type PST, some proportion of the modification could reflect the addition of multiple shorter sialic chains rather than the polymerization of long (>5 units) polysialic acid chains that would be recognized by the OL.28 antibody.

In sum, these data corroborate our OL.28 immunoblot analyses of NCAM polysialylation and the OL.28 immunofluorescence analyses of enzyme autopolysialylation. Mutations in specific PSTD residues decrease both autopolysialylation and NCAM polysialylation to similar extents, whereas replacements of Arg^{82} and Arg^{93}, as well as Glu^{92} and Asp^{94}, in the PBR of PST disproportionately decrease NCAM polysialylation.

DISCUSSION

In this work we have compared two polybasic regions found in the polySTs, PST and STX. The PSTD, or polysialyltransferase domain, is a region enriched in basic residues adjacent to the SMS (Fig. 1*A*). The previous results of Nakata *et al.* (47) were confirmed in this work using a different assay and showed that Lys^{276} and Arg^{277} in the PSTD are particularly important for NCAM polysialylation. Our experiments suggest that replacement of these residues is likely to impact the general catalytic mechanism because both NCAM polysialylation and enzyme autopolysialylation are affected similarly (Figs. 2, 6, and 7). We identified two conserved residues in a second polybasic region we called the PBR that appear to be critical for NCAM polysialylation. In contrast to the PSTD mutations, replacement of Arg^{82} and Arg^{93} in PST or Arg^{97} and Lys^{108} in STX with alanine dramatically reduced NCAM polysialylation and only partially decreased enzyme autopolysialylation. These results suggest that these residues may be required for a productive polyST-NCAM interaction. In PST, replacement of Arg^{93} had the most severe effect on NCAM polysialylation (see Fig. 3), and interestingly, this positively charged residue is surrounded by two negatively charged residues, conserved in only the polySTs (see Fig. 8). Replacement of Glu^{92} and Asp^{94} with alanine largely eliminated the ability of PST to polysialylate NCAM and substantially reduced autopolysialylation (Figs. 5–7), suggesting that they may play a structural role in both maintaining a catalytically active enzyme and in allowing the recognition of the NCAM substrate. Switching these residues in the E92D/D94E mutant surprisingly enhanced enzyme autopolysialyla-

```
ST8Sia I          WRRNQTAARAFRKQMED/CCDPAHLFAMTKMNSPMGK
ST8Sia V          WAMNISEANQFKSTLSR/CCNAPAFLFTTQKNTPLGT
ST8Sia VI         WKRQAEEYANFRAKLAS/CCDAVQNFVVSQNNTPVGT


ST8Sia II(STX)  WRHNQTLSLRIRKQILK/FLDAEKDISVLKGTLKPGD
ST8Sia III      WKFNRTAFLHQRQEILQ/HVDVIKNFSLTKNSVRIGQ
ST8Sia IV(PST)  WKINSSLVLEIRKNILR/FLDAERDVSVVKSSFKPGD
```

FIGURE 8. **Comparison of α2,8-sialyltransferase PBR sequences.** Using the ClustalW and ClustalX version 2 programs (66), we aligned and compared sequences corresponding to the PBR region in PST (ST8Sia IV) and STX (ST8Sia II) for all six α2,8-sialyltransferases. These sequences fell into two groups based on sequence homology. One group contained ST8Sia I, V, and VI, whereas the other contained ST8Sia II/STX, ST8Sia III, and ST8Sia IV/PST. Members of both groups possessed conserved basic residues in the amino-terminal half of this domain (conserved basic residues shown in *bold*). Members of ST8Sia I, V, and VI possessed two adjacent cysteine residues at the beginning of the carboxyl-terminal half of this region, whereas ST8Sia II/STX, ST8Sia III, and ST8Sia IV/PST possessed additional basic residues. Notably, ST8Sia II/STX, ST8Sia III, and ST8Sia IV/PST, which are capable of auto-oligo/polysialylation, have a conserved basic residue corresponding to Arg^{93} in PST, Lys^{112} in ST8Sia III, and Lys^{108} in PST, but only PST Arg^{93} and STX Lys^{108} are flanked by two negatively charged residues (shown in *boldface italic*).

tion but significantly decreased the ability of the enzyme to polysialylate NCAM.

The polymerization of polysialic acid on NCAM glycans is likely to be more complicated than the addition of a single monosaccharide to a growing glycan chain. However, like monoglycosyltransferases, any sequence changes that directly impact the catalytic mechanism either directly or by a change in folding would be expected to eliminate overall activity. In the case of the polySTs, this would be reflected by a decrease in, or elimination of, both NCAM polysialylation and enzyme autopolysialylation. Replacement of residues in the PSTD decreased or eliminated both NCAM polysialylation and enzyme autopolysialylation to the same extent (see comparison in Fig. 7*B*) suggesting that these changes altered the general catalytic activity of PST. The close proximity of the PSTD and particularly Lys^{276} and Arg^{277} to the SMS (see Fig. 1*A*) could have altered the local folding of this region of the protein leading to a decrease in activity or complete inactivation of the enzyme. However, the proper cell surface localization of the mutant proteins suggests that no large changes in folding occurred when these amino acids were replaced (Fig. 2*B*). Replacing the acidic amino acids surrounding Arg^{93} in PST with alanine residues also dramatically decreased the activity of the polyST without a change in trafficking and localization. The possible implications of this will be discussed in more detail below.

Because polysialic acid is found only on a small subset of glycoproteins, this implies a level of substrate specificity that is predicted to involve an initial protein-protein interaction between the polyST and substrate. This idea is supported by evidence from our laboratory that demonstrates the requirement for specific sequences in the NCAM FN1 domain for the polysialylation of *N*-glycans on the adjacent Ig5 domain (13, 15). The ability of the polySTs to polymerize long chains of polysialic acid on substrates adds yet another dimension to this protein-specific modification. We predict that the polymerization of sialic acid is likely to require that the polySTs maintain their interaction with substrates via persistent protein-protein interactions, and that substrate specificity and the ability to polymerize the polysialic acid chain might be achieved by the same polyST-NCAM protein-protein interactions. However, another possibility suggested by Nakata *et al.* (47) is that the polySTs interact with the growing polysialic acid chain and that this allows continued polymerization.

Disruption of sequences in the polySTs required for either binding to NCAM and/or the proper positioning of the polyST may block or decrease NCAM polysialylation without equally impacting polyST autopolysialylation. This is what we have observed when PST Arg^{82} and Arg^{93} and STX Arg^{97} and Lys^{108} are mutated to alanine. On the other hand, amino acid substitutions that decrease or inhibit interaction with the growing polysialic acid chain would be expected to negatively impact both enzyme autopolysialylation and NCAM polysialylation. This is what both Nakata *et al.* (47) and this work show when Lys^{276} and Arg^{277} in the PSTD are replaced. Although it is difficult to discern whether these sequence changes are having a negative impact on catalytic activity or on polysialic acid chain interaction, Nakata *et al.* (47) have demonstrated that the negatively charged glycosaminoglycan, heparin, inhibits the *in vitro* polysialylation of NCAM, providing support for the idea that an enzyme-polysialic acid chain interaction might indeed occur.

Interestingly, we found that acidic residues Glu^{92} and Asp^{94} that flank PST Arg^{93} are critical for enzyme activity and NCAM polysialylation. Replacement of Glu^{92} and Asp^{94} with alanine substantially decreased autopolysialylation (20% of control) and eliminated the ability of the enzyme to polysialylate NCAM (3% of control). In contrast, switching these residues (Glu^{92} to Asp and Asp^{94} to Glu) led to enhanced enzyme autopolysialylation (123% of control) without restoring OL.28 antibody-detectable NCAM polysialylation (Fig. 7). Based on this observation, one wonders whether Glu^{92} and Asp^{94} play an important structural role that is dependent upon interactions that their carboxylic acid side chains make with other amino acids in the structure. Notably, neither mutant was compromised in trafficking out of the ER, suggesting that if a structural change occurred it must have been relatively small and not recognized by the ER quality control system (Fig. 5*B*). The requirement for these specific amino acids flanking Arg^{93} (Glu-Arg-Asp works but Asp-Arg-Glu does not) suggests that the presentation of Arg^{93} could be crucial for NCAM polysialylation and that this might be what is disrupted in the Asp-Arg-Glu mutant.

Secondary structure prediction analysis of the PBR suggests that mutation of Glu^{92} and Asp^{94} may cause structural alterations in the region of Glu^{92}-Arg^{93}-Asp^{94}. The PSIPRED program (55) predicts that the PBR of PST is predominantly helical up to Lys^{100} with a break from Leu^{89} to Asp^{94}. Switching the negative charges of Glu^{92} and Asp^{94} is not predicted to affect the secondary structure. In contrast, replacement of Glu^{92} and Asp^{94} with alanine is predicted to lengthen the helical structure with only a two amino acid break at Leu^{89} and Asp^{90}. However, a second inactive mutant we generated, PST E92K/D94K (data not shown), is not expected to increase the helical content of the PBR, suggesting that altering the structure of Glu^{92}-Arg^{93}-Asp^{94} from a loop to a helix may not be sufficient to abolish PST activity. Another secondary structure prediction program JUFO (56) predicts that the PBR is a combination of unstructured, helical, and strand regions. Glu^{92}-Arg^{93}-Asp^{94} and Asp^{92}-Arg^{93}-Glu^{94} are in a loop beginning at Phe^{88}, with a short

strand beginning at Val^{95}. Replacement of Glu^{92} and Asp^{94} with alanine is predicted to increase the helical content surrounding Ala^{92}-Arg^{93}-Ala^{94}, which itself, unlike in the PSIPRED prediction, remains in a loop. The helix, which in the wild type PBR is expected to end at Arg^{87}, extends as far as Ala^{91} and begins again at Ser^{96} in the mutant, whereas in the wild type sequence a sheet is predicted to begin at Val^{95}. In summary, both programs predict an alteration in the secondary structure of the Ala^{92}-Arg^{93}-Ala^{94} mutant, with an increase in helical content of the PBR. However, they differ on whether the Ala^{92}-Arg^{93}-Ala^{94} mutation itself is in a loop or a helix, so it is difficult to envision a structural model of what is taking place.

In contrast to the changes made in the PSTD, the replacement of specific residues in the PBR led to a decrease or elimination of NCAM polysialylation but notably less dramatic decreases or even enhancement of enzyme autopolysialylation (R82A/R93A and E92D/D94E in particular). This suggested that these changes may alter the protein-protein interactions required for the productive polyST interaction with NCAM. Preliminary co-immunoprecipitation experiments to determine whether replacement of Arg^{82}–Arg^{93} or Glu^{92}-Arg^{93}-Asp^{94} altered the ability of PST to bind to NCAM have given mixed results, and decreases in NCAM binding did not parallel decreases in NCAM polysialylation (data not shown). This leaves the possibility that these residues may be critical for positioning rather than binding *per se*, possibly by forming a second part of a two-part interaction site.

Are charged residues found as part of protein-protein interaction sites? Analyses by several researchers that evaluate the propensity of particular residues at protein interfaces have demonstrated that hydrophobic residues are found most frequently in larger interfaces, with polar residues in higher abundance at smaller interfaces (57). Polar residues are enriched under "hot spots" of binding energy found in protein-protein interfaces and are generally surrounded by rings of hydrophobic residues (58, 59). Tryptophan, arginine, and tyrosine are especially enriched in hot spots with other residues, such as leucine, isoleucine, aspartate, histidine, proline, and lysine, showing some enrichment (59). It is thought that arginine residues are found at high frequency in protein-protein interfaces because the arginine side chain can enter into a variety of noncovalent interactions, including hydrogen bonding, hydrophobic interactions (via its aliphatic side chain carbons), and electrostatic interactions (57, 58, 60). A survey of other protein-specific modification events shows that in some of these the basic amino acids appear to be important for enzyme recognition, as discussed below.

Studies of the mechanisms of protein-specific modification events like the biosynthesis of the mannose 6-phosphate recognition marker of lysosomal enzymes, and the addition of GalNAc-4-sulfate to the termini of pituitary glycoprotein hormones, have focused on identifying regions in the substrates recognized by the specific enzymes rather than the reverse. In both cases, positively charged amino acids have been identified as important components of the recognition regions of these substrates. Specifically placed lysine and arginine residues are critical for the phosphorylation of the high mannose glycans of lysosomal enzymes and other proteins like DNase I that carry mannose 6-phosphate residues. These basic residues are part of a surface patch on the substrate that is recognized by the *N*-acetylglucosamine-1-phosphotransferase (61–63). The α-subunit of pituitary glycoprotein hormones and other proteins, like carbonic anhydrase VI, that have GalNAc-4-sulfate rather than Gal-sialic acid at the terminus of their *N*-glycans contain a stretch of amino acids rich in lysine residues that are recognized by the *N*-acetylgalactosaminyltransferases. Recently, Miller *et al.* (64) demonstrated that a 19-amino acid sequence from the carboxyl terminus of carbonic anhydrase-VI is necessary and sufficient for recognition by two β1,4-GalNAc transferases and allows them to add β1,4-linked GalNAc to the termini of the *N*-glycans of a reporter protein. A stretch of basic residues (KRKKEK) in this sequence is critical but not completely sufficient for recognition. This basic sequence is similar to the PLRSKK sequence that forms an α-helix in the α-subunit of pituitary glycoprotein hormones and is critical for recognition by the pituitary β1,4-GalNAc transferase (65).

A comparison of the sequences spanning the PBR of all six α2,8-sialyltransferases (ST8Sia enzymes), using ClustalW and ClustalX version 2 (66), demonstrates that they partition into two groups that differ both in the number of basic amino acids and in common sequences in the carboxyl-terminal half of this region (Fig. 8). The polySTs, STX (ST8Sia II) and PST (ST8Sia IV), and ST8Sia III, an enzyme that is capable of auto-oligo/polysialylation but that is not able to recognize and polysialylate NCAM (46), form one group. ST8Sia I, V, and VI that add monosialic acid to substrates form the second group. The polySTs and ST8Sia III have a higher overall number of basic residues (5–9 basic residues) than do the other three sialyltransferases (2–4 basic residues). However, what is most striking is that the sequences of these two groups of enzymes are significantly different in the carboxyl-terminal half of the PBR in several respects. ST8Sia I, V, and VI possess two adjacent cysteine residues not found in PST, STX, and ST8Sia III, whereas these latter enzymes have three conserved basic residues that are missing from the sequences of STSia I, V, and VI (only one lysine is found in ST8Sia I) (Fig. 8). But most notably, ST8Sia III contains a Lys at the same position as Arg^{93} in PST and Lys^{108} in STX, but it lacks the acidic residues surrounding this residue (Glu and Asp) that are absolutely conserved in the two polySTs. The conservation of the acidic-basic-acidic motif coupled with the results of our mutagenesis studies allow us to suggest that these residues may be critical for a productive polyST-NCAM interaction. Future structural work is needed to confirm our predictions.

Acknowledgments—We are grateful to Dr. Eric Vimr for providing us with the protocol and plasmid for the expression and purification of the K1E endoneuraminidase N. We also thank Drs. Jack Kaplan and Arnon Lavie for insightful suggestions and discussions about the work.

REFERENCES

1. Kojima, N., Yoshida, Y., Kurosawa, N., Lee, Y.-C., and Tsuji, S. (1995) *FEBS Lett.* **360,** 1–4
2. Eckhardt, M., Muhlenhoff, M., Bethe, A., Koopman, J., Frosch, M., and Gerardy-Schahn, R. (1995) *Nature* **373,** 715–718
3. Nakayama, J., Fukuda, M. N., Fredette, B., Ranscht, B., and Fukuda, M.

(1995) *Proc. Natl. Acad. Sci. U. S. A.* **92,** 7031–7035
4. Scheidegger, E. P., Sternberg, L. R., Roth, J., and Lowe, J. B. (1995) *J. Biol. Chem.* **270,** 22685–22688
5. Finne, J., Finne, U., Deagostini-Bazin, H., and Gordis, C. (1983) *Biochem. Biophys. Res. Commun.* **112,** 482–487
6. Rothbard, J. B., Brackenbury, R., Cunningham, B. A., and Edelman, G. M. (1982) *J. Biol. Chem.* **257,** 11064–11069
7. James, W. M., and Agnew, W. S. (1987) *Biochem. Biophys. Res. Commun.* **148,** 817–826
8. Zuber, C., Lackie, P., Catterall, W., and Roth, J. (1992) *J. Biol. Chem.* **267,** 9965–9971
9. Yabe, U., Sato, C., Matsuda, T., and Kitajima, K. (2003) *J. Biol. Chem.* **278,** 13875–13880
10. Curreli, S., Arany, Z., Gerardy-Schahn, R., Mann, D., and Stamatos, N. M. (2007) *J. Biol. Chem.* **282,** 30346–30356
11. Close, B. E., and Colley, K. J. (1998) *J. Biol. Chem.* **273,** 34586–34593
12. Muhlenhoff, M., Eckhardt, M., Bethe, A., Frosch, M., and Gerardy-Schahn, R. (1996) *EMBO J.* **15,** 6943–6950
13. Close, B. E., Mendiratta, S. S., Geiger, K. M., Broom, L. J., Ho, L. L., and Colley, K. J. (2003) *J. Biol. Chem.* **278,** 30796–30805
14. Mendiratta, S. S., Sekulic, N., Hernandez-Guzman, F. G., Close, B. E., Lavie, A., and Colley, K. J. (2006) *J. Biol. Chem.* **281,** 36052–36059
15. Mendiratta, S. S., Sekulic, N., Lavie, A., and Colley, K. J. (2005) *J. Biol. Chem.* **280,** 32340–32348
16. Cunningham, B. A., Hemperly, J. J., Murray, B. A., Prediger, E. A., Brackenbury, R., and Edelman, G. M. (1987) *Science* **236,** 799–806
17. Nelson, R. W., Bates, P. A., and Rutishauser, U. (1995) *J. Biol. Chem.* **270,** 17171–17179
18. Angata, K., Nakayama, J., Fredette, B., Chong, K., Ranscht, B., and Fukuda, M. (1997) *J. Biol. Chem.* **272,** 7182–7190
19. Ong, E., Nakayama, J., Angata, K., Reyes, L., Katsuyama, T., Arai, Y., and Fukuda, M. (1998) *Glycobiology* **8,** 415–424
20. Hildebrandt, H., Becker, C., Murau, M., Gerardy-Schahn, R., and Rahmann, H. (1998) *J. Neurochem.* **71,** 2339–2348
21. Kiss, J. Z., Troncoso, E., Djebbara, Z., Vutskits, L., and Muller, D. (2001) *Brain Res. Rev.* **36,** 175–184
22. Oltmann-Norden, I., Galuska, S. P., Hildebrandt, H., Geyer, R., Gerardy-Schahn, R., Geyer, H., and Muhlenhoff, M. (2008) *J. Biol. Chem.* **283,** 1463–1471
23. Phillips, G. R., Krushel, L. A., and Crossin, K. L. (1997) *Dev. Brain Res.* **102,** 143–155
24. Johnson, C. P., Fujimoto, I., Rutishauser, U., and Leckband, D. E. (2005) *J. Biol. Chem.* **280,** 137–145
25. Yang, P., Major, D., and Rutishauser, U. (1994) *J. Biol. Chem.* **269,** 23039–23044
26. Yang, P., Yin, X., and Rutishauser, U. (1992) *J. Cell Biol.* **116,** 1487–1496
27. Weinhold, B., Seidenfaden, R., Rockle, I., Muhlenhoff, M., Schertzinger, F., Conzelmann, S., Marth, J. D., Gerardy-Schahn, R., and Hildebrandt, H. (2005) *J. Biol. Chem.* **280,** 42971–42977
28. Livingston, B. D., Jacobs, J. L., Glick, M. C., and Troy, F. A. (1988) *J. Biol. Chem.* **263,** 9443–9448
29. Hildebrandt, H., Becker, C., Gluer, S., Rosner, H., Gerardy-Schahn, R., and Rahmann, H. (1998) *Cancer Res.* **58,** 779–784
30. Suzuki, M., Nakayama, J., Suzuki, A., Angata, K., Chen, S., Sakai, K., Hagihara, K., Yamaguchi, Y., and Fukuda, M. (2005) *Glycobiology* **15,** 887–894
31. Komminoth, P., Roth, J., Lackie, P. M., Bitter-Suermann, D., and Heitz, P. U. (1991) *Am. J. Pathol.* **139,** 297–304
32. Tanaka, F., Otake, Y., Nakagawa, T., Kawano, Y., Miyahara, R., Li, M., Yanagihara, K., Nakayama, J., Fujimoto, I., Ikenaka, K., and Wada, H. (2000) *Cancer Res.* **60,** 3072–3080
33. Gluer, S., Schelp, C., Gerardy-Schahn, R., and von Schweinitz, D. (1998) *J. Pediatr. Surg.* **33,** 1516–1520
34. Roth, J., Zuber, C., Wagner, P., Taatjes, D. J., Weiserber, C., Heitz, P. U., Gordis, C., and Bitter-Suermann, D. (1988) *Proc. Natl. Acad. Sci. U. S. A.* **85,** 2999–3003
35. Roth, J., Zuber, C., Wagner, P., Blaha, I., Bitter-Suermann, D., and Heitz, P. U. (1988) *Am. J. Pathol.* **133,** 227–240
36. Livingston, B. D., and Paulson, J. C. (1993) *J. Biol. Chem.* **268,** 11504–11507
37. Drickamer, K. (1993) *Glycobiology* **3,** 2–3
38. Geremia, R. A., Harduin-Lepers, A., and Delannoy, P. (1997) *Glycobiology* **7,** v–xi
39. Datta, A. K., and Paulson, J. C. (1995) *J. Biol. Chem.* **270,** 1497–1500
40. Datta, A. K., Sinha, A., and Paulson, J. C. (1998) *J. Biol. Chem.* **273,** 9608–9614
41. Kitazume-Kawaguchi, S., Kabata, S., and Arita, M. (2001) *J. Biol. Chem.* **276,** 15696–15703
42. Jeanneau, C., Chazalet, V., Auge, C., Soumpasis, D. M., Harduin-Lepers, A., Delannoy, P., Imberty, A., and Breton, C. (2004) *J. Biol. Chem.* **279,** 13461–13468
43. Kapitonov, D., Bieberich, E., and Yu, R. K. (1999) *Glycoconj. J.* **16,** 337–350
44. Kapitonov, D., and Yu, R. K. (1999) *Glycobiology* **9,** 961–978
45. Angata, K., Chan, D., Thibault, J., and Fukuda, M. (2004) *J. Biol. Chem.* **279,** 25883–25890
46. Angata, K., Suzuki, M., McAuliffe, J., Ding, Y., Hindsgaul, O., and Fukuda, M. (2000) *J. Biol. Chem.* **275,** 18594–18601
47. Nakata, D., Zhang, L., and Troy, F. A. (2006) *Glycoconj. J.* **23,** 423–436
48. Sevigny, M. B., Ye, J., Kitazume-Kawaguchi, S., and Troy, F. A., II (1998) *Glycobiology* **8,** 857–867
49. Close, B. E., Tao, K., and Colley, K. J. (2000) *J. Biol. Chem.* **275,** 4484–4491
50. Bonner, W. M., and Lasky, R. A. (1974) *Eur. J. Biochem.* **46,** 83–88
51. Steenbergen, S. M., Lee, Y. C., Vann, W. F., Vionnet, J., Wright, L. F., and Vimr, E. R. (2006) *J. Bacteriol.* **188,** 6195–6206
52. Pelkonen, S., Pelkonen, J., and Finne, J. (1989) *J. Virol.* **63,** 4409–4416
53. Close, B. E., Wilkinson, J. M., Bohrer, T. J., Goodwin, C. P., Broom, L. J., and Colley, K. J. (2001) *Glycobiology* **11,** 997–1008
54. Sato, C., Fukuoka, H., Ohta, K., Matsuda, T., Koshino, R., Kobayashi, K., Troy, F. A., and Kitajima, K. (2000) *J. Biol. Chem.* **275,** 15422–15431
55. Jones, D. T. (1999) *J. Mol. Biol.* **292,** 195–202
56. Meiler, J., and Baker, D. (2003) *Proc. Natl. Acad. Sci. U. S. A.* **100,** 12105–12110
57. Glaser, F., Steinberg, D. M., Vakser, I. A., and Ben-Tai, N. (2001) *Proteins Struct. Funct. Genet.* **43,** 89–102
58. Bogan, A. A., and Thorn, K. S. (1998) *J. Mol. Biol.* **280,** 1–9
59. Ma, B., Elkayam, T., and Nussinov, R. (2003) *Proc. Natl. Acad. Sci. U. S. A.* **100,** 5772–5777
60. Janin, J., Miller, S., and Chothia, C. (1988) *J. Mol. Biol.* **204,** 155–164
61. Nishikawa, A., Gregory, W., Frenz, J., Cacia, J., and Kornfeld, S. (1997) *J. Biol. Chem.* **272,** 19408–19412
62. Baranski, T. J., Koelsch, G., Hartsuck, J. A., and Kornfeld, S. (1991) *J. Biol. Chem.* **266,** 23365–23372
63. Steet, R., Lee, W. S., and Kornfeld, S. (2005) *J. Biol. Chem.* **280,** 33318–33323
64. Miller, E., Fiete, D., Blake, N. M., Beranek, M., Oates, E. L., Mi, Y., Roseman, D. S., and Baenziger, J. U. (2008) *J. Biol. Chem.* **283,** 1985–1991
65. Mengeling, B. J., Manzella, S. M., and Baenziger, J. U. (1995) *Proc. Natl. Acad. Sci. U. S. A.* **92,** 502–506
66. Larkin, M. A., Blackshields, G., Brown, N. P., Chenna, R., McGettigan, P. A., McWilliam, H., Valentin, F., Wallace, I. M., Wilm, A., Lopez, R., Thompson, J. D., Gibson, T. J., and Higgins, D. G. (2007) *Bioinformatics* (*Oxf.*) **23,** 2947–2948